Available online www.jsaer.com

***Journal of Scientific and Engineering Research*, 2021, 8(10):106-116**

Research Article

ISSN: 2394-2630
CODEN(USA): JSERBR

Behavior Study of Heterojunction Based on $CuInS_2/CuInSe_2$ Solar Cell in Two and Three Dimensional Representations under Monochromatic Light Illumination from Near Infrared to Visible: n^+n/pp^+ Model

E.M. Keita, Y. Tabar, M.S. Mane, M. Dia, C. Sene, B. Mbow

Laboratoire des Semiconducteurs et d'Energie Solaire, Département de Physique, Faculté des Sciences et Techniques, Université Cheikh Anta Diop, Dakar, Sénégal
Corresponding author: elouazy@hotmail.fr

Abstract In this paper, we study behavior of thin films solar cells of heterojunctions type n^+n/pp^+ based on $CuInSe_2$ and $CuInS_2$, under monochromatic illumination. The structure $ZnO(n^+)/CdS(n)/CuInS_2(p)/CuInSe_2(p^+)$ is considered where $CuInS_2$ represent the base and $CuInSe_2$ the substrate. ZnO and CdS are used as window layers. The evolution of the internal quantum efficiency is represented by varying some electrical and geometric parameters of the structure [1]. In this work, we study particularly, generation rate and photo-generated minority carrier densities profiles versus junction depth, for different illuminations. These parameters are studied in two and three dimensions representation. We consider the range from near infrared to visible, photon energies ranging between 1.04 eV (λ = 1.192 μm) and 3.1 eV (λ = 0.4 μm). The profiles study of these intrinsic parameters allows to better explain and understand the behavior of the spectral response, to locate the losses within the structure, to visualize the behavior of carriers at the interfaces and to study the effect of the latter on the collection efficiency for photovoltaic applications.

Keywords Thin films, $CuInS_2$ and $CuInSe_2$, spectral response, generation rate, carrier densities

Introduction

$CuInS_2$ and $CuInSe_2$ are two materials belonging to the family of inorganic chalcopyrite semiconductors. They have fairly similar lattice parameters [2-11] and different energy band gaps. In this work we propose to study theoretically under monochromatic illuminations, the behavior of the n^+n/pp^+ type decreasing band gap heterostructure, defined by the model $ZnO(n^+)/CdS(n)/CuInS_2(p)/CuInSe_2(p^+)$ where ZnO and CdS layers are used as wide energy band gap window layers, $CuInS_2$ is used as a base and $CuInSe_2$ as a substrate. It involves studying the intrinsic parameters such as the generation rate and the photo-generated minority carrier densities. The internal quantum efficiency depends on the profiles of these parameters. The study of these parameters allows to visualize the behavior of the photo-created carriers in the different regions of the structure, to identify the influence of the electrical and geometric parameters on the collection efficiency, shows the transport direction of the carriers and the effects of the interfaces and surfaces on their collection.

Materials and Methods

Models of theoretical calculations based on the continuity equation governing carrier transport in semiconductor materials and the effects of optical absorption coefficient, geometric and electrical parameters of the different materials are proposed to establish the expressions of these intrinsic parameters (generation rate and photo-generated minority carrier densities) and the spectral response. We neglect the optical reflection coefficient at each interface in the spectral range used. It is also considered that the space charge region is located only

between the n and p regions and there is no electric field outside this region. We neglect recombination phenomena in the space charge region.

In figures 1 we represent the optical absorption coefficients of the different materials and the ZnO reflection coefficient [2, 9, 10, 12]. The diagram of the structure is shown in figure 2 and the energy band diagram is represented in figure 3 [1].

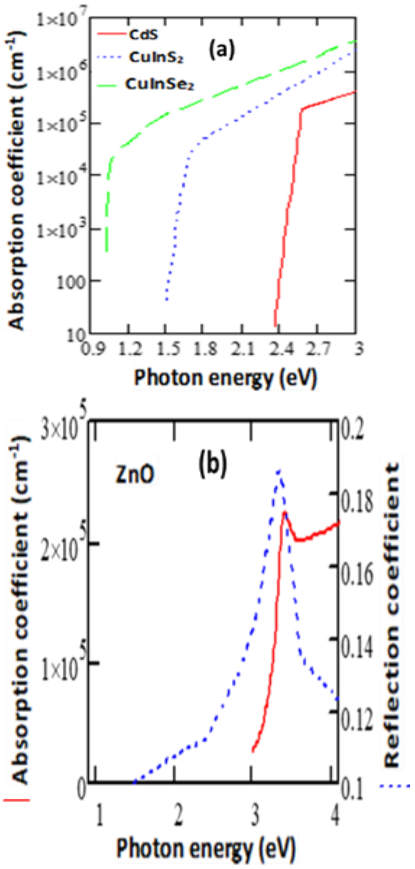

Figure 1: (a) Absorption coefficient of CdS, $CuInS_2$, $CuInSe_2$ materials versus photon energy [2, 9 - 10] ; (b) Absorption coefficient and reflection coefficient of ZnO material versus photon energy [12]

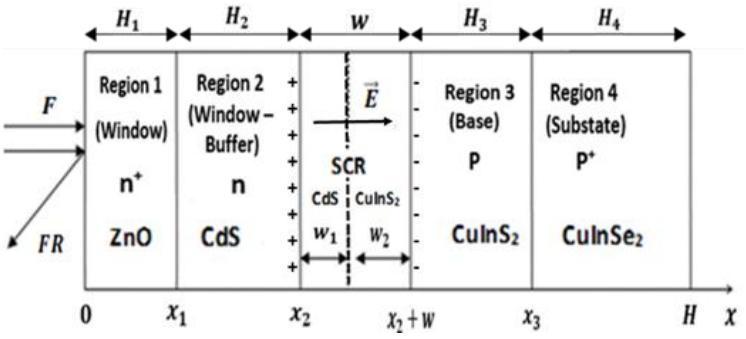

Figure 2: Diagram of the structure $ZnO(n^+)/CdS(n)CuInS_2(p)/CuInSe_2(p^+)$

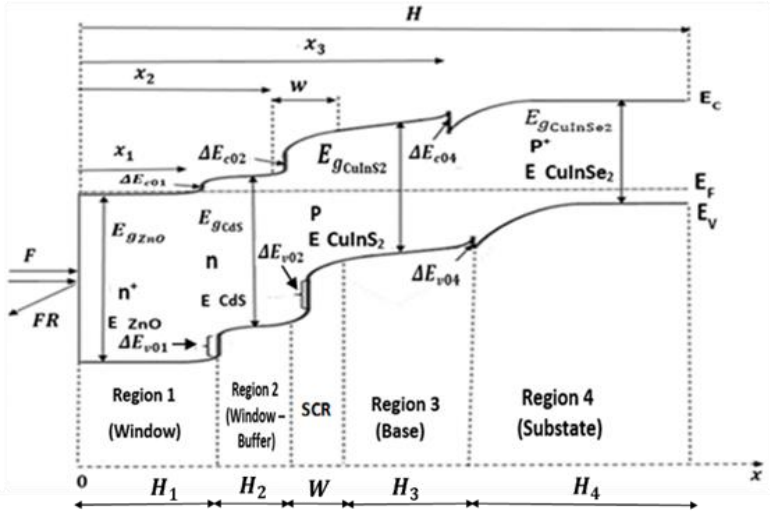

Figure 3: Energy band diagram of the structure $ZnO(n^+)/CdS(n)/CuInS_2(p)/CuInSe_2(p^+)$[1]

Density of photo-generated holes in region 1

In region 1 (ZnO layer), $0 \le x \le x_1$, the photocurrent is essentially due to the holes, the continuity equation is written :

$$\frac{d^2\Delta p_1}{dx^2} - \frac{\Delta p_1}{{L_{p_1}}^2} = \frac{-\alpha_1 F(1-R)e^{-\alpha_1 x}}{D_{p_1}} \quad (1)$$

With ${L_{p_1}}^2 = D_{p_1}\tau_{p_1}$ (2)

The expression of the generation rate is given by : $G_1(x) = \alpha_1 F(1-R)e^{-\alpha_1 x}$ (3)

Boundary conditions are given by [9, 10, 13] :

$$D_{p_1}\left(\frac{d\Delta p_1}{dx}\right) = S_{p_1}\Delta p_1 \quad \text{for} \quad x = 0 \quad (4)$$

$$\Delta p_1 = 0 \quad \text{for} \quad x = x_1 \quad (5)$$

The solution of equation (1) gives the expression of the density of photo-created holes in region 1, it is written:

$$\Delta p_1(x) = -\frac{\alpha_1 {L_{p_1}}^2 F(1-R)}{D_{p_1}(\alpha_1^2 {L_{p_1}}^2 - 1)} \cdot \left[e^{-\alpha_1 \cdot x} + \frac{\left(\frac{S_{p_1}L_{p_1}}{D_{p_1}} + \alpha_1 L_{p_1}\right)\cdot \mathrm{sh}\left(\frac{x-H_1}{L_{p_1}}\right) - e^{-\alpha_1 H_1}\left[\frac{S_{p_1}L_{p_1}}{D_{p_1}}\mathrm{sh}\left(\frac{x}{L_{p_1}}\right) + \mathrm{ch}\left(\frac{x}{L_{p_1}}\right)\right]}{\frac{S_{p_1}L_{p_1}}{D_{p_1}}sh\left(\frac{H_1}{L_{p_1}}\right) + ch\left(\frac{H_1}{L_{p_1}}\right)} \right] \quad (6)$$

Density of photo-generated holes in region 2

In region 2 (CdS layer), $x_1 \le x \le x_2$, the photocurrent is also a hole current. The interface effects are characterized by a recombination velocity at the interface noted S_{p_2}. The continuity equation is given by :

$$\frac{d^2\Delta p_2}{dx^2} - \frac{\Delta p_2}{{L_{p_2}}^2} = \frac{-\alpha_2 F(1-R)e^{-\alpha_1 H_1}e^{-\alpha_2(x-H_1)}}{D_{p_2}} \quad (7)$$

With $${L_{p_2}}^2 = D_{p_2}\tau_{p_2} \quad (8)$$

The expression of the generation rate is given by : $G_2(x) = \alpha_2 F(1-R)e^{-\alpha_1 H_1}e^{-\alpha_2(x-H_1)}$ (9)

Boundary conditions are given by [9, 10, 14, 15] :

$$D_{p_2}\frac{d\Delta p_2}{dx} = S_{p_2}\Delta p_2 + D_{p_1}\frac{d\Delta p_1}{dx} \quad \text{for} \quad x = x_1 \quad (10)$$

$$\Delta p_2 = 0 \quad \text{for} \quad x = x_2 \quad (11)$$

The solution of equation (7) gives the density of photo-created holes in region 2, it is given by :

$$\Delta p_2(x) = -\frac{\alpha_2 {L_{p_2}}^2 F(1-R)e^{-\alpha_1 H_1}}{D_{p_2}\left(\alpha_2{}^2 {L_{p_2}}^2 - 1\right)} \cdot \left[e^{-\alpha_2(x-H_1)} + \frac{\left(\frac{S_{p_2}L_{p_2}}{D_{p_2}} + \alpha_2 L_{p_2}\right)\cdot \mathrm{sh}\left(\frac{x-(H_1+H_2)}{L_{p_2}}\right)}{\frac{S_{p_2}L_{p_2}}{D_{p_2}}sh\left(\frac{H_2}{L_{p_2}}\right) + ch\left(\frac{H_2}{L_{p_2}}\right)} - \right.$$

$$\left. \frac{e^{-\alpha_2 H_2}\left[\frac{S_{p_2}L_{p_2}}{D_{p_2}}\mathrm{sh}\left(\frac{x-H_1}{L_{p_2}}\right) + \mathrm{ch}\left(\frac{x-H_1}{L_{p_2}}\right)\right]}{\frac{S_{p_2}L_{p_2}}{D_{p_2}}sh\left(\frac{H_2}{L_{p_2}}\right) + ch\left(\frac{H_2}{L_{p_2}}\right)} \right] - \frac{\mathrm{sh}\left(\frac{x-(H_1+H_2)}{L_{p_2}}\right)\cdot\ \alpha_1 F(1-R)L_{p_1}L_{p_2}}{D_{p_2}(\alpha_1^2 {L_{p_1}}^2 - 1)\left\{\frac{S_{p_2}L_{p_2}}{D_{p_2}}sh\left(\frac{H_2}{L_{p_2}}\right) + ch\left(\frac{H_2}{L_{p_2}}\right)\right\}} \times$$

$$\left\{ \frac{\left(\frac{S_{p_1}L_{p_1}}{D_{p_1}} + \alpha_1 L_{p_1}\right) - e^{-\alpha_1 H_1}\left[\frac{S_{p_1}L_{p_1}}{D_{p_1}}ch\left(\frac{H_1}{L_{p_1}}\right) + sh\left(\frac{H_1}{L_{p_1}}\right)\right]}{\frac{S_{p_1}L_{p_1}}{D_{p_1}}sh\left(\frac{H_1}{L_{p_1}}\right) + ch\left(\frac{H_1}{L_{p_1}}\right)} - \alpha_1 L_{p_1}e^{-\alpha_1 H_1} \right\} \quad (12)$$

Density of photo-generated electrons in the substrate (region 4)

In region 4, the substrate ($CuInSe_2$), the photocurrent is due to the electrons, the continuity equation is given by :

$$\frac{d^2\Delta n_4}{dx^2} - \frac{\Delta n_4}{L_{n_4}^2} = \frac{-\alpha_4}{D_{n_4}}F(1-R)e^{-\alpha_1 H_1}e^{-\alpha_2(H_2+w_1)}e^{-\alpha_3(H_3+w_2)}e^{-\alpha_4[x-(H-H_4)]} \quad (13)$$

The expression of the generation rate is given by :

$$G_4(x) = \alpha_4 F(1-R)e^{-\alpha_1 H_1}e^{-\alpha_2(H_2+w_1)} \times e^{-\alpha_3(H_3+w_2)}e^{-\alpha_4[x-(H-H_4)]} \quad (14)$$

Boundary conditions are given by [9, 10, 13] :

$$D_{n_4}\frac{d\Delta n_4}{dx} = -S_{n_4}\Delta n_4 \quad \text{for} \quad x = H \quad (15)$$

$$\Delta n_4 = 0 \quad \text{for} \quad x = x_3 \quad (16)$$

The density of photo-created electrons in region 4 (substrate: $CuInSe_2$) is solution of equation (13), It is given by:

$$\Delta n_4(x) = -\frac{\alpha_4 {L_{n_4}}^2 F(1-R)e^{[(\alpha_2-\alpha_1)H_1]}}{D_{n_4}\left(\alpha_4{}^2 {L_{n_4}}^2 - 1\right)} \times e^{[(\alpha_3-\alpha_2)(H_1+H_2+w_1)]}e^{[(\alpha_4-\alpha_3)(H-H_4)]} \times \left[e^{-\alpha_4 x} + \right.$$

$$\left. \frac{\left(\alpha_4 L_{n_4} - \frac{S_{n_4}L_{n_4}}{D_{n_4}}\right)e^{-\alpha_4 H}\cdot \mathrm{sh}\left(\frac{x-(H-H_4)}{L_{n_4}}\right)}{\frac{S_{n_4}L_{n_4}}{D_{n_4}}sh\left(\frac{H_4}{L_{n_4}}\right) + ch\left(\frac{H_4}{L_{n_4}}\right)} - \frac{e^{-\alpha_4(H-H_4)}\left[\frac{S_{n_4}L_{n_4}}{D_{n_4}}\mathrm{sh}\left(\frac{H-x}{L_{n_4}}\right) + \mathrm{ch}\left(\frac{H-x}{L_{n_4}}\right)\right]}{\frac{S_{n_4}L_{n_4}}{D_{n_4}}sh\left(\frac{H_4}{L_{n_4}}\right) + ch\left(\frac{H_4}{L_{n_4}}\right)} \right] \quad (17)$$

Density of photo-generated electrons in the base (region 3)

In region 3, the base ($CuInS_2$ layer), $x_2 + w \le x \le x_3$, the photocurrent is also due to the electrons. The interface effects are characterized by a recombination velocity at the interface noted S_{n_3}. The continuity equation is given by :

$$\frac{d^2\Delta n_3}{dx^2} - \frac{\Delta n_3}{L_{n_3}^2} = \frac{-\alpha_3}{D_{n_3}}F(1-R)e^{-\alpha_1 H_1}e^{-\alpha_2(H_2+w_1)}e^{-\alpha_3[x-(H_1+H_2+w_1)]} \quad (18)$$

The expression of the generation rate is given by:

$$G_3(x) = \alpha_3 F(1-R)e^{-\alpha_1 H_1}e^{-\alpha_2(H_2+w_1)} \times e^{-\alpha_3[x-(H_1+H_2+w_1)]} \quad (19)$$

Boundary conditions can be written as [1]:

$$\Delta n_3 = 0 \quad \text{for} \quad x = x_2 + w \quad (20)$$

$$D_{n_3}\frac{d\Delta n_3}{dx} = -S_{n_3}\Delta n_3 + D_{n_4}\frac{d\Delta n_4}{dx} \quad \text{for} \quad x = x_3 \quad (21)$$

The density of photo-created electrons in region 3 (base : $CuInS_2$), is solution of equation (18), It is given by :

$$\Delta n_3(x) = -\frac{\alpha_3 {L_{n_3}}^2 F(1-R) e^{[(\alpha_2-\alpha_1)H_1]} e^{[(\alpha_3-\alpha_2)(H_1+H_2+w_1)]}}{D_{n_3}\left(\alpha_3^2 {L_{n_3}}^2-1\right)} \times \left[e^{-\alpha_3 x} + \frac{\left(\alpha_3 L_{n_3} - \frac{S_{n_3} L_{n_3}}{D_{n_3}}\right) e^{-\alpha_3 (H-H_4)} \cdot \mathrm{sh}\left[\frac{x-(H_1+H_2+w)}{L_{n_3}}\right]}{\frac{S_{n_3} L_{n_3}}{D_{n_3}} sh\left[\frac{H_3}{L_{n_3}}\right] + ch\left[\frac{H_3}{L_{n_3}}\right]} - \right.$$

$$\left. \frac{e^{-\alpha_3 (H_1+H_2+w)}\left[\frac{S_{n_3} L_{n_3}}{D_{n_3}} \cdot \mathrm{sh}\left(\frac{(H-H_4)-x}{L_{n_3}}\right) + \mathrm{ch}\left(\frac{(H-H_4)-x}{L_{n_3}}\right)\right]}{\frac{S_{n_3} L_{n_3}}{D_{n_3}} sh\left[\frac{H_3}{L_{n_3}}\right] + ch\left[\frac{H_3}{L_{n_3}}\right]} \right] - \frac{\mathrm{sh}\left[\frac{x-(H_1+H_2+w)}{L_{n_3}}\right] \alpha_4 L_{n_4} L_{n_3} F(1-R) e^{[(\alpha_2-\alpha_1)H_1]}}{D_{n_3}\left(\alpha_4^2 {L_{n_4}}^2-1\right)\left\{\frac{S_{n_3} L_{n_3}}{D_{n_3}} sh\left[\frac{H_3}{L_{n_3}}\right] + ch\left[\frac{H_3}{L_{n_3}}\right]\right\}} \times$$

$$e^{[(\alpha_3-\alpha_2)(H_1+H_2+w_1)]} e^{[(\alpha_4-\alpha_3)(H-H_4)]} \times \left[\frac{\left(\alpha_4 L_{n_4} - \frac{S_{n_4} L_{n_4}}{D_{n_4}}\right) e^{-\alpha_4 H}}{\frac{S_{n_4} L_{n_4}}{D_{n_4}} sh\left(\frac{H_4}{L_{n_4}}\right) + ch\left(\frac{H_4}{L_{n_4}}\right)} + \frac{e^{-\alpha_4 (H-H_4)}\left[\frac{S_{n_4} L_{n_4}}{D_{n_4}} \cdot \mathrm{ch}\left(\frac{H_4}{L_{n_4}}\right) + \mathrm{sh}\left(\frac{H_4}{L_{n_4}}\right)\right]}{\frac{S_{n_4} L_{n_4}}{D_{n_4}} sh\left(\frac{H_4}{L_{n_4}}\right) + ch\left(\frac{H_4}{L_{n_4}}\right)} - \right.$$

$$\left. \alpha_4 L_{n_4} e^{-\alpha_4 (H-H_4)} \right] \qquad (22)$$

By noting :

$$J_{R1-R2} = -qD_{p_2} \left.\frac{d\Delta p_2}{dx}\right|_{x=x_2} \qquad (23)$$

$$J_{B-Sub} = qD_{n_3} \left.\frac{d\Delta n_3}{dx}\right|_{x=x_2+w} \qquad (24)$$

$$J_{SCR} = -qF(1-R)e^{-\alpha_1 H_1}\left\{e^{-\alpha_2 H_2} \times [e^{-\alpha_2 w_1} - 1] + e^{-\alpha_2 (H_2+w_1)} \times [e^{-\alpha_3 w_2} - 1]\right\} \qquad (25)$$

J_{SCR} is the photocurrent due to generated carriers in the space charge region [1].

The internal quantum efficiency (or spectral response) IQE is given by [9, 10, 14, 16]:

$$\mathrm{IQE} = \frac{J_{R1-R2} + J_{SCR} + J_{B-Sub}}{qF(1-R)} \qquad (26)$$

Results & Discussion

Spectral response graphs for different parameters

Figure 4-a shows the internal quantum efficiency (or spectral response) versus photon energy for different thicknesses of the base or region 3 ($CuInS_2$ layer) H_3, the diffusion length in the base is fixed at L_{n_3} = 3 µm and the recombination velocity at the interface base-substrate is fixed at $S_{n_3} = 2 \times 10^5$cm.s^{-1}. In Figure 4-b we represent the internal quantum efficiency versus photon energy for different diffusion lengths of electrons in the base L_{n_3}, the thickness of the base is fixed at H_3 =1 µm and the recombination velocity at the interface base-substrate is fixed at $S_{n_3} = 2 \times 10^5$cm.s^{-1}. These graphs (figures 4-a, 4-b) show the influence of the structure parameters (thickness, diffusion length) on the collection efficiency.

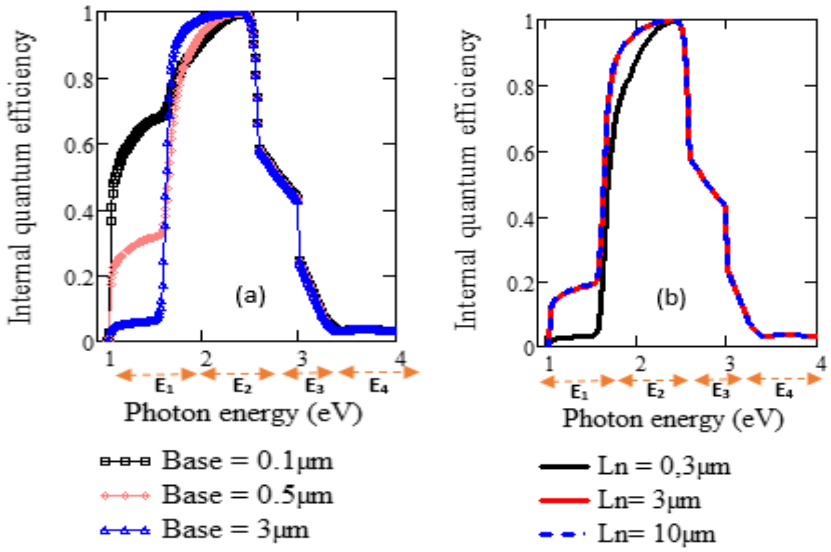

Figure 4: Internal quantum efficiency vs. photon energy (a) for different thicknesses of the base (region 3: $CuInS_2$ layer); (b) for different diffusion lengths of electrons in the base (region 3: $CuInS_2$ layer);

(s_{p_1} =2 × 10^7 $cm.s^{-1}$; H_1 = 0.3 μm; L_{p_1} = 0.4 μm ; s_{p_2} =2 × 10^4 $cm.s^{-1}$; H_2 = 0.1 μm; L_{p_2} = 0.5 μm ; s_{n_3} =2 × 10^5 $cm.s^{-1}$; H_3 = 1 μm (b); L_{n_3} = 3 μm (a); s_{n_4} =2 × 10^7 $cm.s^{-1}$; L_{n_4} = 1 μm ; W_1 = 0.02 μm ; W_2 = 0.08 μm ;W = 0.1 μm ; H = 100 μm ; $D_{p_1} = 0.51cm^2.s^{-1}$; $D_{p_2} = 0.64cm^2.s^{-1}$; $D_{n_3} = 5.13cm^2.s^{-1}$; $D_{n_4} = 10.27cm^2.s^{-1}$)

In Figure 5-a, we represent the internal quantum efficiency versus thickness of the base H_3 for different radiation energies ranging between 1.1 eV (λ = 1.127 μm) and 2.48 eV (λ = 0.5 μm). The diffusion length is fixed at L_{n_3} = 3 μm. We note that for a radiation energy lower than the energy band gap of the base ($CuInS_2$ layer), E <1.57 eV, the efficiency decreases with the base thickness's and does not exceed 65% for the considered parameters. Indeed, for E <1.57 eV, photons are only absorbed by the substrate ($CuInSe_2$ layer), its contribution to the internal quantum efficiency increases by reducing the base thickness's, this phenomenon is also illustrated on Figure 4-a (part E_1).

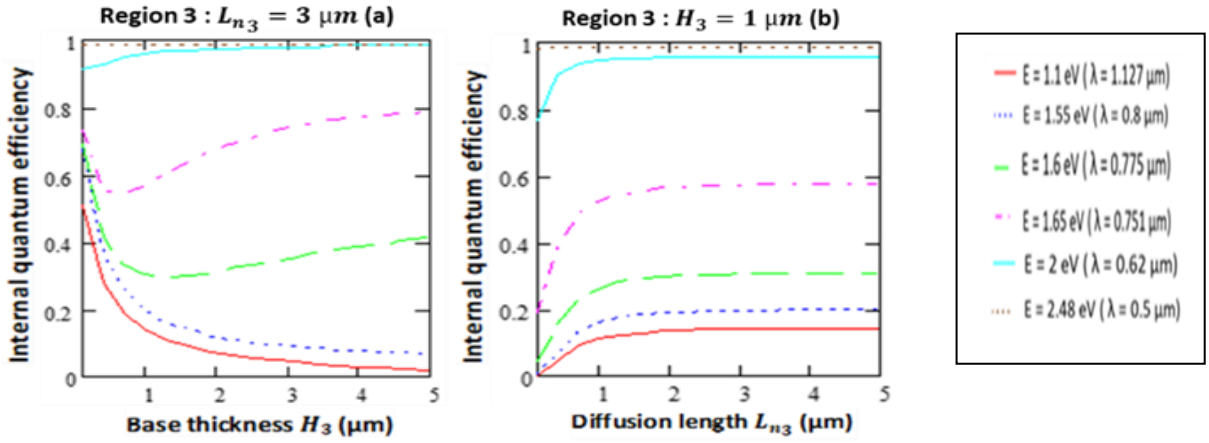

Figure 5: (a) Internal quantum efficiency vs. thickness of the base (region 3 : $CuInS_2$ layer); (b) Internal quantum efficiency vs. diffusion length of electrons in the base (region 3 : $CuInS_2$ layer);
(s_{p_1} =2 × 10^7 $cm.s^{-1}$; H_1 = 0.3 μm; L_{p_1} = 0.4 μm ; s_{p_2} =2 × 10^4 $cm.s^{-1}$; H_2 = 0.1 μm; L_{p_2} = 0.5 μm ; s_{n_3} =2 × 10^5 $cm.s^{-1}$ (a) and (b) ; H_3 = 1 μm (b) and (c) ; L_{n_3} = 3 μm (a) and (c) ; s_{n_4} =2 × 10^7 $cm.s^{-1}$; L_{n_4} = 1 μm ; W_1 = 0.02 μm ; W_2 = 0.08 μm ;W = 0.1 μm ; H = 100 μm ; $D_{p_1} = 0.51cm^2.s^{-1}$; $D_{p_2} = 0.64cm^2.s^{-1}$; $D_{n_3} = 5.13cm^2.s^{-1}$; $D_{n_4} = 10.27cm^2.s^{-1}$)

For photon energies ranging between 1.57 eV and 2 eV, greater than the energy band gap of the base ($CuInS_2$ layer), the internal quantum efficiency firstly decreases with base thickness's, reaches a minimum value (the minimum value is approximately equal to 35% for E = 1.6 eV (λ = 0.775 μm) and 56% for E = 1.65 eV (λ = 0.751 μm)) and secondly increases with the base thickness's. The decreasing phase indicates that photons are mostly absorbed by the substrate and the increasing phase shows that the base and the space charge region mainly absorb the incident photons.

Figure 5-b shows the variation of the internal quantum efficiency versus diffusion length of electrons in the base L_{n_3} for different values of the radiation energy, the thickness of the base is fixed at H_3 = 1 μm and the recombination velocity at the base-substrate interface at $S_{n_3} = 2 \times 10^5 cm.s^{-1}$. We note that for each radiation energy, the efficiency firstly increases with the diffusion length, reaches a maximum value and then becomes constant for $L_{n_3} > H_3$.On the other hand, we note that the efficiency increases with the radiation energy lower than the energy band gap of window layers ZnO (3.1 eV) and CdS (2.5 eV). It shows that the contribution of the rear areas (space charge region, base and substrate) to the efficiency increases with photon energy.

For radiation energy ranging between 2 eV and 2.5 eV, all photons are practically absorbed by the space charge region (CdS (0.02 μm)/$CuInS_2$ (0.08 μm)) and a thin thickness of the base ($CuInS_2$), the internal quantum

efficiency is close to 100%. The thickness of the base, the diffusion length and the recombination velocity at the interface become less influential on the collection efficiency (figures 5-a, 5-b).

Study of the behavior of the structure under monochromatic light illumination

In this part, we study in the case of monochromatic illuminations, the profiles of the generation rate and the photo-generated minority carriers versus junction depth.

We consider radiation energies ranging between 1.04 eV (λ = 1.192 µm) and 3.1 eV (λ = 0.4 µm). We consider the following parameters in table 1:

Table 1: Physical parameters considered for monochromatic illumination

Region i	H_i (µm)	L_{p_i}, L_{n_i} (µm)	S_{p_i}, S_{n_i} $(cm.s^{-1})$	μ_{p_i}, μ_{n_i} $(cm^2/V.s)$	D_{p_i}, D_{n_i} $(cm^2.s^{-1})$
ZnO (n^+) (Region 1)	0.3	0.3	2×10^7	20	0.51
CdS (n) (Region 2)	0.1	0.4	2×10^4	25	0.64
$CuInS_2$ (p) (Region 3: Base)	1	3	2×10^5	200	5.13
$CuInSe_2$ (p^+) (Region 4: Substrate)	98.5	1	2×10^7	400	10.27

$w_1 = 0.02\mu m$; $w_2 = 0.08\mu m$; $H = 100\mu m$

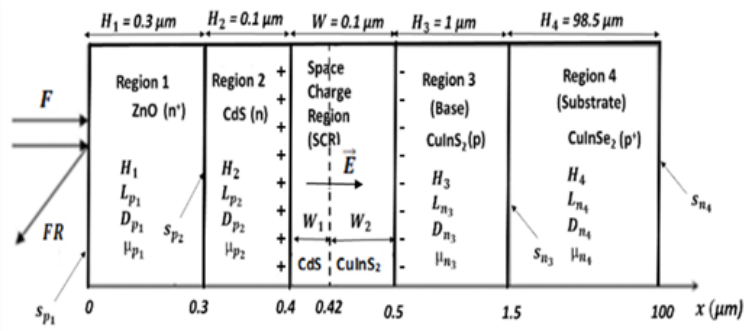

Figure 6: Diagram of the structure with considered parameters

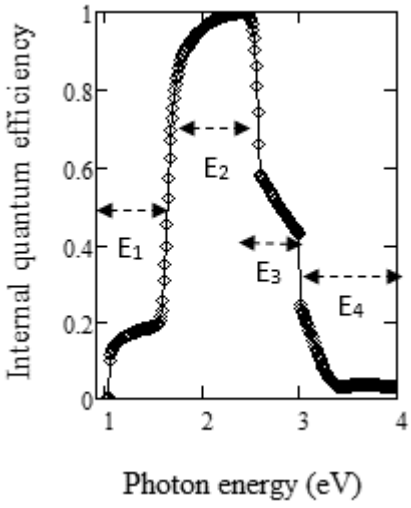

Figure 7: Internal quantum efficiency vs. photon energy

Internal quantum efficiency

Figure 7 shows the internal quantum efficiency for the considered parameters in table 1. Part E_4 (E <1.57 eV) shows the contribution of the substrate, it is less than 20%, many carriers generated in the substrate are lost, these losses are caused by the interface effects ($S_{n_3} = 2 \times 10^5 cm.s^{-1}$). Part E_2 (1.57 eV <E <2.4 eV) shows the contributions of the base and the space charge region. The contribution of the base is also affected by carrier losses at the base-substrate interface. The contribution of the space charge region is important, it does not depend on the interface effects. There maximum contribution exceeds 90% for photon energy neighboring 2.3 eV. Parts E_3 and E_4 show the absorption of photons by the frontal layers (CdS and ZnO) above 2.5 eV. Absorption of photons by these frontal layers reduces the overall efficiency, it is due to carrier losses by recombination phenomenon at the frontal surface ($S_{p_1} = 2 \times 10^7 cm.s^{-1}$) and at the ZnO /CdS interface ($S_{p_2} = 2 \times 10^4 cm.s^{-1}$) [1] .

Monochromatic illumination

Profile of the generation rate

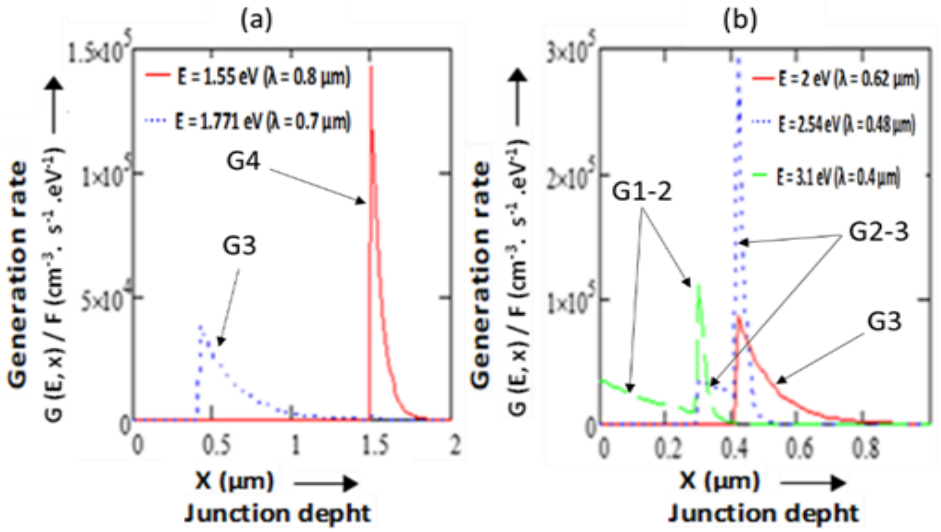

Figure 8: (a and b) Generation rate vs. junction depth (x) under monochromatic illumination

In Figures 8-a and 8-b, we represent the profile of the generation rate versus junction depth (x) for radiation energies ranging between 1.1 eV (1.127 µm) and 3.1 eV (0.4 µm). On each graph we note that the generation rate decreases with the thickness when the radiation energy reaches the energy band gap of the material. A radiation energy lower than the energy band gap of the material causes no carrier generation. Photons having energy ranging between 1.04 eV and 1.57 eV are only absorbed by the substrate (or $CuInse_2$ layer) for x> 1.5 µm. Figure 8-a shows for E = 1.55 eV (λ = 0.8 µm) the graph of the generation rate in the substrate (curve G4). Photons having energy E = 1.771 eV (λ = 0.7 µm) and E = 2 eV (λ = 0.62 µm), chosen arbitrarily, are absorbed only by the $CuInS_2$ layer (curves G3) for 0.42 µm ≤x ≤1.5 µm (base and region w_2 of the space charge region). For E = 2.54 eV (λ = 0.8 µm), chosen arbitrarily, the graph of the generation rate shows two peaks (curve G2-3) for 0.3 µm ≤x≤ 0.5 µm. The first peak at x = 0.3 µm is due to the photon absorption by CdS layer and the second at x = 0.42 µm to the photon absorption by $CuInS_2$ layer. For E = 3.1 eV (λ = 0.4 µm), chosen arbitrarily, the generation rate is due to the absorption of photons by ZnO layer and CdS layer (curve G1-2) for for 0 µm ≤x≤ 0.3 µm

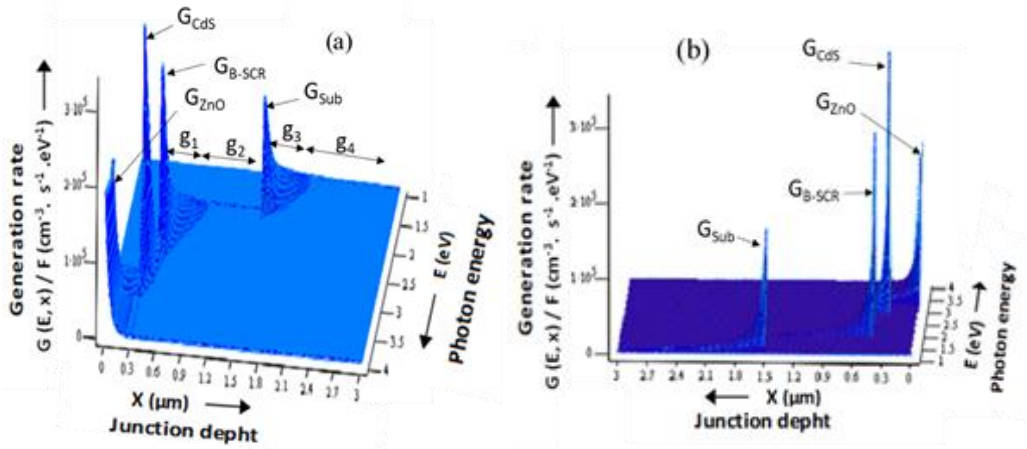

Figure 9: (a and b) Three-dimensional representation of generation rate vs. photon energy and junction depth (x) under monochromatic illumination : figures (a) and (b) are identical only the view angles differ

Figures 9-a and 9-b show the profile of the generation rate represented simultaneously versus the photon energy and the junction depth of the structure, it is a representation in three dimensions. The two figures are identical, only the angles of view differ. We obtain four peaks (signals) modeling the four materials used. The signal obtained between 1 eV and 1.57 eV (signal G_{Sub}) corresponds to the absorption of photons by the substrate (or

$CuInSe_2$ layer), it is mostly located between 1.5 µm and 2 µm (part g3), beyond 2 µm the signal is low indicating that the majority of the photons does not reach this area (part g4), They are absorbed on a thin thickness in order of 0.5 µm (part g3). The signal obtained between 1.57 eV and 2.5 eV (signal $G_{B\text{-}SCR}$) corresponds to the absorption of photons by the base and the space charge region (or $CuInS_2$ layer) and is mainly located between 0.42 µm and 0.9 µm (part g1). This signal is low between 0.9 µm and 1.5 µm (part g2), the carriers are therefore absorbed on a thin thickness of $CuInS_2$ layer in order of 0.5 µm. The signal obtained between 2.5 eV and 3 eV (signal G_{CdS}) is due to the absorption of photons by the region 2 and the space charge region (or CdS layer), it is located between 0.3 µm and 0.42 µm The signal obtained between 3 eV and 4 eV (signal G_{ZnO}) corresponds to the absorption of photons by region 1 (or ZnO layer), it is localized between 0 µm and 0.3 µm.

Profiles of minority carrier densities

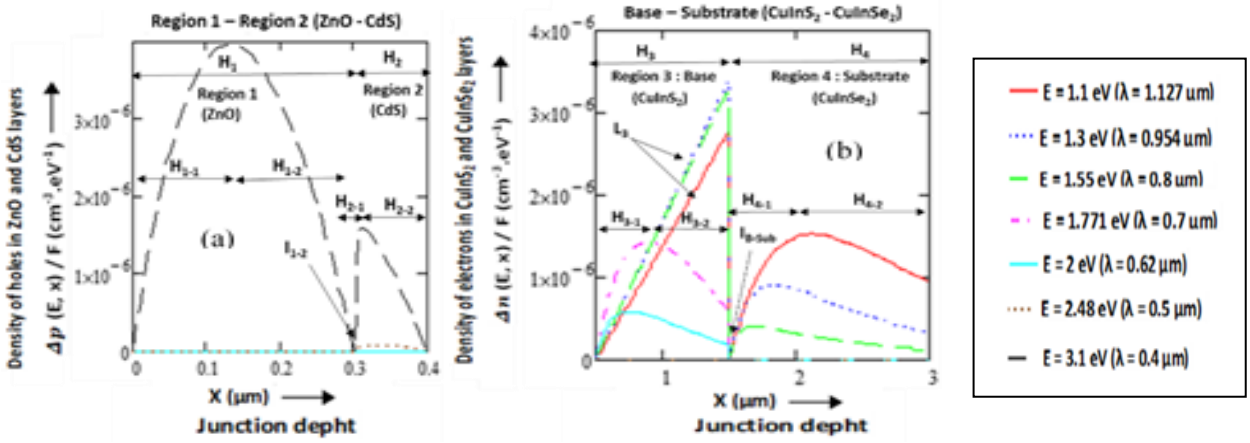

Figure 10: Density of minority carriers photocreated vs. junction depth (x) under monochromatic illumination: a) density of holesin regions 1 and 2 (ZnO-CdS); b) density of electrons in regions 3 and 4 (base and substrate: $CuInS_2$ – $CuInSe_2$)

In Figure 10-a, we represent the profile of the holes generated versus thickness of the frontal layers (ZnO and CdS: 0 µm≤x≤0.4 µm) for different radiation energies. The hole density is zero in the non-absorption range of ZnO and CdS (E ≤2.5 eV). For a radiation energy equal to 3.1 eV, arbitrarily chosen, photons are absorbed by ZnO layer (part H_1) and CdS layer (part H_2). Carrier losses observed at the ZnO surface (part H_{1-1}) and at the ZnO-CdS interface I_{1-2} (part H_{2-1}) reduce the density of holes in the CdS layer (part H_2). These losses of carriers explain the drastic decrease of the spectral response beyond 3 eV (part E_4 figures 4 and 7).

Figure 10-b) shows the electron density profile versus the thickness of the base (or $CuInS_2$ layer : part H_3) and the substrate (or $CuInSe_2$ layer : part H_4) for different radiation energies. Photons having energy lower than 1.57 eV ($CuInS_2$ energy band gap), absorbed only by the substrate generate an electron density distribution with a linear profile in the base (curves L_3), they all diffuse toward the collection area (space charge region). This linear profile of electron density, causes a decrease of the resulting diffusion photocurrent when the thickness of the base increases even if the diffusion length is sufficient ($L_{n_3} > H_3$). This linear profile explains also the decrease of the substrate contribution in the spectral response by increasing the thickness of the base (figure 4-a, part E_1). In the substrate (part H_4) some photo-created electrons are also lost at the base-substrate interface I_{B-Sub} by recombination phenomenon ($S_{n_3} = 2 \times 10^5 \text{cm.s}^{-1}$) and in volume by diffusing towards the back surface (part H_{4-2}). The carrier losses at the base-substrate interface (I_{B-Sub}) also explain the decrease of electron density for E = 1.771 eV (λ = 0.7 µm) and E = 2 eV (λ = 0.62 µm) observed in the base near the interface (part H_{3-2}). These carrier losses related to the interface effects (I_{B-Sub}, part H_{3-2}), to the diffusion of carriers towards the back surface of the substrate (part H_{4-2}), to the decrease of the diffusion photocurrent of carriers generated by the substrate due to the increase of base thickness (curves L_3), explain the low contribution of the substrate to the internal quantum efficiency which does not exceed 20% for $S_{n_3} = 2 \times 10^5 \text{cm.s}^{-1}$and $H_3 = 1\mu\text{m}$ (figure 4-b and figure 7, part E_1).

Three-dimensional representation of minority carrier density profiles

Minority carrier density profiles studied in figures 10-a and 10-bare represented in three dimensions in figures 11 and 12. They are represented simultaneously versus photon energy and junction depth of the structure.

- Figures 11-a and 11-b represent the density of holes generated in the ZnO (part H_1) and in the CdS (part H_2) layers. The figures are identical only the angles of view differ. The cavity observed around 3.3 eV (C) shows a high losses of carriers in ZnO layer, it also corresponds to a high generation rate of carriers. These graphs summarize the figure 10-a in three-dimensional representation.

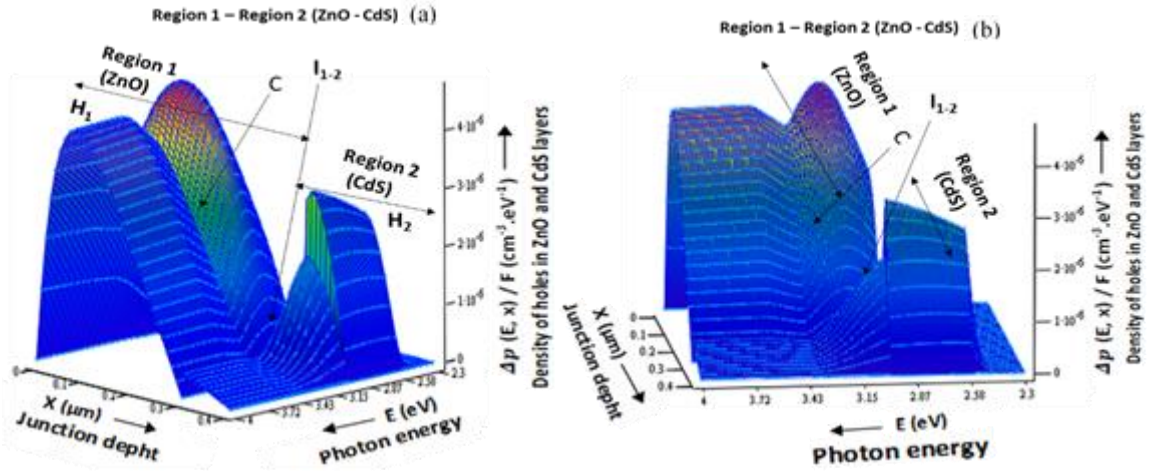

Figure 11: Three-dimensional representation density of holes vs. photon energy and junction depth (x) under monochromatic illumination in regions 1 and 2 (ZnO-CdS): figures (a) and (b) are identical only the view angles differ

- Figures 12-a and 12-b show the electron density in the base and the substrate. The figures are identical only the angles of view differ. Each figure has two signals, the one observed in the range 0.5 µm ≤ x ≤ 1.5 µm (part H_3) corresponds to the density of electrons in the base ($CuInS_2$), the signal obtained for x > 1. 5 µm (part H_4) represents the density of those generated in the substrate ($CuInSe_2$). The discontinuity of the electron density profile observed at x = 1.5 µm locates the base-substrate interface (I_{B-Sub},). These graphs summarize the figure 10-b in three-dimensional representation.

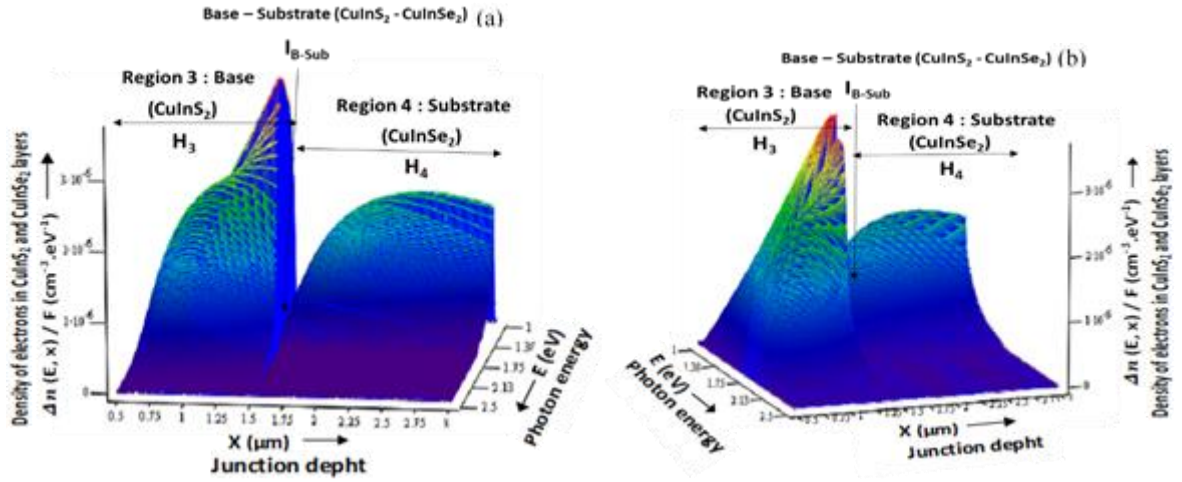

Figure 12: Three-dimensional representation density of electrons vs. photon energy and junction depth (x) under monochromatic illumination in regions 3 and 4 (base and substrate : $CuInS_2$ – $CuInSe_2$) : figures (a) and (b) are identical only the view angles differ

Conclusion

In this work, the four-layer structure $ZnO(n^+)/CdS(n)/CuInS_2(p)/CuInSe_2(p^+)$ (model $n^+/n/p/p^+$), whose materials are arranged by decreasing energy band gap , is considered. The substrate and the base are different materials,

they impose boundary conditions that take into account phenomena or states of the interface. We have studied behavior of the structure under monochromatic illuminations in order to optimize performances for a better functioning.

For this study, on the one hand, the internal quantum efficiency has been represented by varying some geometrical and electrical parameters (base thickness's and diffusion length). As we have used window layers in the frontal area (ZnO and CdS), the variation of the parameters concerns only the rear area (base and substrate: $CuInS_2$, $CuInSe_2$). The results obtained show that the spectral response essentially depends on these parameters and their optimization is essential for a best collection of carriers and a better performance of the structure.

On the other hand, to study the intrinsic behavior of the structure, we have represented the generation rate and the minority carrier density profiles of holes and electrons for different illuminations, in two and three dimensions, taking into account junction depth and photon energy. These intrinsic parameters are at the origin of the spectral response curves. These studies allow to visualize the behavior of the different areas of the structure, to identify the influence of the parameters on the collection of the carriers and to locate the carrier losses by recombination in volume, surface and interface. Thus, it allows to find the best geometric dimensions and electrical parameters to optimize the efficiency of the solar cell.

Nomenclature:

F : Incident photons flux($cm^{-2}.s^{-1}$)
R : Reflection coefficient of region 1 (ZnO)
H : Thickness of the structure (μm)
w_1 : Thickness of CdS layer in the space charge region (SCR) (μm)
w_2 : Thickness of $CuInS_2$ layer in the space charge region (SCR) (μm)
w : Thickness of the space charge region (μm)
q : Elementary charge ($1.6 \times 10^{-19} C$)

Layer / Parameter	ZnO (n^+) (Region 1)	CdS (n) (Region 2)	$CuInS_2$ (p) (Region 3: Base)	$CuInSe_2$ (p^+) (Region 4: Substrate)
Minority carriers	Holes (p)	Holes (p)	Electrons (n)	Electrons (n)
Absorption coefficient (cm^{-1})	α_1	α_2	α_3	α_4
Diffusion coefficient $cm^2.s^{-1}$	D_{p_1}	D_{p_2}	D_{n_3}	D_{n_4}
Lifetime (μs)	τ_{p_1}	τ_{p_2}	τ_{n_3}	τ_{n_4}
Diffusion length (μm)	L_{p_1}	L_{p_2}	L_{n_3}	L_{n_4}
Recombination velocity (surface or interface) ($cm.s^{-1}$)	S_{p_1}	S_{p_2}	S_{n_3}	S_{n_4}
Thickness (μm)	H_1	H_2	H_3	H_3
Generatioon rate ($cm^{-3}.s^{-1}$)	G_1	G_2	G_3	G_4
Density (electrons or holes) (cm^{-3})	Δp_1	Δp_2	Δn_3	Δn_4

References

[1]. E.M. Keita, B. Ndiaye, M. Dia, Y. Tabar, C. Sene, B. Mbow, '' Theoretical Study of Spectral Responses of Heterojunctions Based on $CuInSe_2$ and $CuInS_2$ ''OAJ Materials and Devices, Vol 5#1, 0508(2020) – DOI: 10.23647/ca.md20200508

[2]. Subba Ramaiah Kodigala, ''$Cu(In_{1-x}Ga_x)se_2$ based thin solar cells'', 2010, Volume 35, Academic Press, ELSEVIER. Inc, p. 16.

[3]. T. Loher, W. Jaegermann, C. Pettenkofer, '' Formation and electronic properties of the $CdS/CuInSe_2$ (011) heterointerface studied by synchrotron-induced photoemission'', J. Appl. Phys. 77 (1995) 731.

[4]. H. Hahn, G. Frank, W. Klinger, A.D. Meyer, G. Strorger, '' Über einige ternäre Chalkogenide mit Chalcopyritestruktur'', Z. Anorg. Aug. Chem. 271 (1953) 153.

[5]. M. Robbins, V.G. Lambrecht Jr., '' Preparation and some properties of materials in systems of the type $M^IM^{III}S_2$ / $M^IM^{III}Se_2$ where M^I = Cu, Ag and M^{III} = Al, Ga, In'', Mater. Res. Bull. 8 (1973) 703.

[6]. I.V. Bodnar, B.V. Korzun, A.I. Lukomski, '' Composition Dependence of the Band Gap of $CuInS_{2x}Se_{2(1-x)}$'', Phys. Stat. Solidi (B) 105 (1981) K143.

[7]. S.J. Fonash, Solar Cell device Physics, Academic Press, New York, 1981.

[8]. H.L. Hwang, C.Y. Sun, C.Y. Leu, C.C. Cheng, C.C. Tu, '' Growth of $CuInS_2$ and its characterization'', Rev. Phys. Appl. 13 (1978) 745.

[9]. E.M. Keita, B. Mbow, M.S. Mane, M.L. Sow, C. Sow, C. Sene ''Theoretical Study of Spectral Responses of Homojonctions Based on CuInSe2'' Journal of Materials Science & Surface Engineering, Vol. 4 (4), 2016, pp392-399.

[10]. E.M. Keita *, B. Mbow, M.L. Sow , C. Sow, M. Thiam , C. Sene, '' Theoretical Comparative Study of Internal Quantum Efficiency of Thin Films Solar Cells Based on $CuInSe_2$: $p^+/p/n/n^+$, $p/n/n^+$, $p^+/p/n$ and p/n MODELS'' INTERNATIONAL Journal of Engineering Sciences & Research Technology, 5(9): September, 2016, 344-359

[11]. S. B. Zhang, Su-Huai Wei, and Alex Zunger, '' Stabilization of Ternary Compounds via Ordered Arrays of Defect Pairs'', Phys. Rev. Lett, 1997, vol. 78, 4059

[12]. Hisashi Yoshikawa, Sadao Adachi,''Optical Constants of ZnO'', Jpn. J.Appl. Phys. Vol 36 (1997) pp.6237-6243.

[13]. B. Mbow, A. Mezerreg, N. Rezzoug, and C. Llinares, ''Calculated and Measured Spectral Responses in Near-Infrared of III-V Photodetectors Based on Ga, In, and Sb'', phys. Stat. Sol. (a) 141, 511 (1994).

[14]. H. J. Hovel and J. M. Woodall,'' $Ga_{1-x}Al_xAs$ - GaAs P-P-N Heterojunction Solar Cells'', J. Electrochem. Soc. 120, 1246 (1973).

[15]. H. J. Hovel and J. M. Woodall, 10^{th} IEEE Photovoltaic Specialists Conf., Palo Alto (Calif.) 1973 (p.25).

[16]. H. J. Hovel, "Semiconductors and Semimetals: Solar Cells'', 11, Academic Press, New York, 127 (1975).